Towards a better understanding of debris flow sediment sources: Monitoring of an active rock slope at Spitze Stei, Switzerland

Małgorzata Chmiel[1*], *Lena* Husmann[1], *Fabian* Walter[1], *Huw* Horgan[2], *Giacomo* Belli[3], *Emanuele* Marchetti[3], and *Christian* Kienholz[4]

[1] Swiss Federal Institute for Forest, Snow and Landscape Research WSL, Birmensdorf, Switzerland
[2] WSL Institute for Snow and Avalanche Research SLF, Davos, Switzerland
[3] Department of Earth Sciences, University of Firenze, Firenze, Italy
[4] GEOTEST AG, Zollikofen, Switzerland

Abstract. Rapid process cascades can lead to destructive debris flows. Identifying and characterizing the processes conditioning debris-flow occurrence will strongly contribute to the mitigation of debris-flow hazards. In recent years, the rock slope near "Spitze Stei", in the Kandersteg region, Switzerland, has exhibited elevated displacement rates exceeding 10 cm per day, suggesting a growing instability up to 20 million m^3. The accumulated sediments at the bottom of the Spitze Stei slope are mobilized as debris flows by melting snow and heavy summer precipitations. Here, we use seismology combined with an intelligent algorithm to automatically detect rockfall and landslides at the Spitze Stei rock slope. These mass movements act as primary sediment sources delivering sediments to a debris-prone channel. Our initial results quantify mass movement activity before two debris flow events that occurred in 2022 and identify their triggers. Such analysis can contribute towards mitigating debris flow hazards and extending warning time, especially for debris flows triggered by factors other than precipitation.

1 Introduction

Catastrophic debris flows might result from a rapid process cascade [1, 2]. An initial event such as a rock/ice avalanche [1] can cause a downstream chain reaction that can be particularly far-reaching, especially when large amounts of water are involved, as in the case of debris flows. Such events are relatively rare but might happen suddenly and have severe consequences. Limited understanding of the mechanism of individual processes and process interactions makes cascading mass movements particularly challenging to integrate into natural hazard management. Identifying the initial source of sediments and studying the processes conditioning debris-flow occurrence will strongly contribute to debris-flow hazard mitigation.

Here, by combining seismology and machine learning, we study the gravitational sediment transport from the Spitze Stei rockslide to a debris-prone channel, Oeschibach. Spitze Stei is a large-scale slope instability located in Switzerland in the Kandersteg region (Figure 1).

2 Spitze Stei

The Spitze Stei rockslide extends over ~0.5 km² in elevation between 2200 and 2900 m a.s.l. The area of

Spitze Stei has a history of catastrophic rock avalanches that repeatedly occurred throughout the Holocene, with volumes reaching hundreds of million m³ [3]. At the Spitze Stei slope, the current displacement rates are several meters per year, seasonally exceeding 10 cm per day [4].
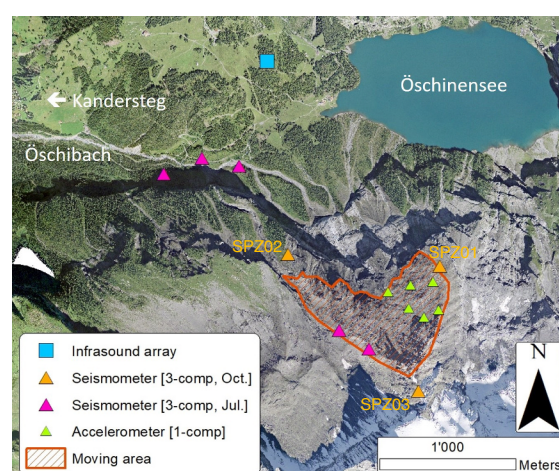
Fig. 1. Study site at Spitze Stei, Switzerland, and seismo-infrasonic installations. The Spitze Stei slope is outlined with the orange line.

This suggests a growing instability of up to 20 million m³ [5]. Despite the high displacement rates, until

---

* Corresponding author: malgorzata.chmiel@wsl.ch

now, mostly minor debris avalanches and rockfalls (volumes in the order of several 1,000 m^3 up to 10,000-15,000 m^3, Figure 2) have occurred at Spitze Stei [6].

Due to the destructive potential of the Spitze Stei rockslide, extensive monitoring has been put in place since 2018 [7]. Borehole temperature, geophysical measurements, and direct observations underline the presence of degrading permafrost, particularly on planes of enhanced gliding and shear deformation [4]. The slope consists of different sectors with various deformation rates and directions, favoring the scenario of a material collapse through multiple large (0.6-1M m^3) rockfalls and debris avalanches [8, 9].

2.1 Debris Flows at Oeschibach

Processes occurring at Spitze Stei can be divided into primary and secondary [4, 5]:

1. Primary processes occur directly at the slope and involve the breaking and sliding of slope material (rockfalls and landslides).
2. The secondary processes are triggered by the material of the primary processes, which develop from accumulated debris in the Oeschibach bed at the terminus of the slope (e.g., sediment transporting floods and debris flows).

The frequency and volume of the debris flows are directly related to the primary processes at Spitze Stei [10]. If the Spitze Stei activity ceases, no major floods or debris flows are expected. On the other hand, an increased mass movement activity can cause large debris flows that flow might endanger the village of Kandersteg [10]. Since the beginning of 2020, preventive measurements have been created around the Oeschibach channel, including the construction of a retention dam. The Oeschibach stream has been monitored with discharge measurements, automatic cameras, and drone flights. So far, the debris flows have reached volumes ranging from several 1,000 to ~15,000 m^3.

The debris flows at Oeschibach are triggered by meltwater, melt of snow deposits, and heavy rainfall [10]. Without precipitation, debris flows are usually more granular and have smaller volumes. The number of debris flow events in 2018 and 2019 is unclear; 3 and 8 were reported in 2021 and 2021, respectively [10].
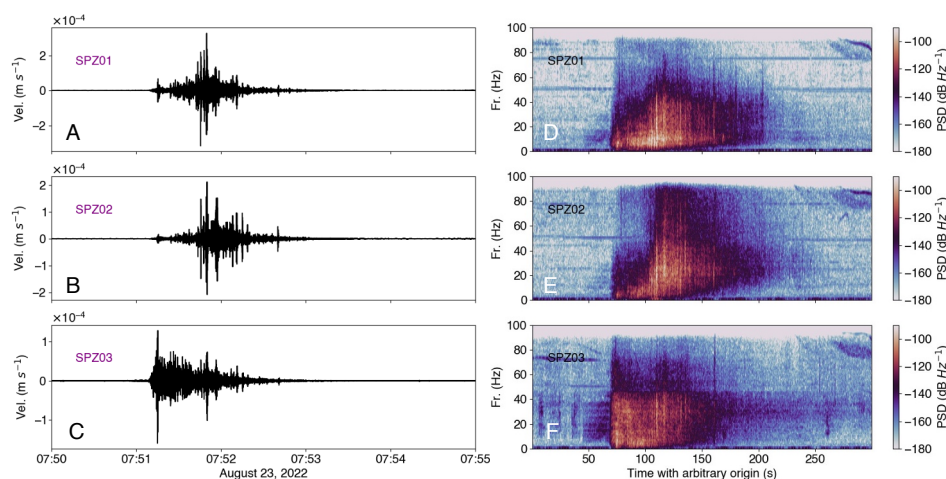
Fig. 2. Seismic signals of a debris avalanche as Spitze Stei that occurred on August 23, 2022, at 07:51:10 UTC (volume ~8,000 m^3). Panels A, B, and C show seismic signals with the corresponding spectrograms (D, E, and F) recorded at stations SPZ01, SPZ02, and SPZ03.

3 Data and methods

In October 2021, we installed three 3-component seismometers directly at the slope that continuously recorded seismic signals. An infrasound array with four microphones was also installed ~1,500 m in front of the slope terminus to strengthen mass-movement detection. In summer 2022, we locally densified the acquisition with ten more seismic sensors deployed near the slope and close to the Oeschibach channel (Figure 1). The sensors' location was chosen based on the proximity to primary and secondary processes, terrain accessibility, and azimuthal and spatial coverage of the areas impacted by the processes.

Climatic factors (such as rain, temperature changes, and freezing-thawing cycles) can cause mechanical changes within the slope that affect the rock slope stability [11]. Seismic waves that propagate within the slope are sensitive to these mechanical changes, and we can measure the changes through seismic interferometry [12]. Mass movements generate both infrasonic and seismic waves as air is pushed aside by an accelerating mass and as particles impact the Earth surface, respectively. The seismic and infrasound signals allow us to detect the mass-movement events and characterize their source mechanism [13].

3.1 Machine Learning detection of mass movements at Spitze Stei

We use seismic data combined with an intelligent algorithm to automatically detect mass movements

occurring at the Spitze Stei slope. With this approach, we aim to quantify the activity of primary processes (rockfall and landslides) at Spitze Stei that condition the debris flow activity in the Oeschibach channel. To detect rockfalls and landslides at Spitze Stei, we use a supervised machine learning approach based on Random Forest [14, 15, 16].

In the following, we summarize the methods; the details can be found in [17]. The idea is to develop a classifier that will automatically distinguish between seismic signals of noise and mass movements recorded at stations SPZ01, SPZ02, and SPZ03 (Figure 1, orange triangles). To do so, we first compile an initial catalog of mass movements and noise signals that will be used to train the classifier. We use the infrasound array to identify mass movement signals that might originate from the Spitze Stei rockslide between October and December 2021. The infrasound array automatically identifies coherent acoustic signals and provides their back-azimuth. We use the back-azimuth information to identify potential occurrences of mass movements at Spitze Stei and confirm them through visual validation.

We then include signals from helicopters, earthquakes, rainfall, and anthropogenic noise in the noise class. We also include randomized noise signal samples from the entire year to correctly represent seasonal variations in ambient noise signals. The final catalog includes 17 h of the mass movement signals and 39.5 h of the noise signals. We then divide these signals into discrete time windows of 10 s to further increase the training dataset. With that, the number of noise time windows amounts to 28,476, and mass movement time windows to 12,276.

We describe the seismic data through 69 features that describe signals' waveform, spectral properties, and how the signal's coherent properties vary spatially over the three stations. After training and validating the machine learning model, we apply it to the continuous seismic data recorded at stations SPZ01, SPZ02, and SPZ03. This provides us with time series of classification per station. We define "detections" when a machine learning classifier indicates the mass movement class.

We apply the following post-processing steps to stabilize the results of the detection:
1. We require the detections to be confirmed by at least 2 seismic stations, including the top station SPZ03.

2. To focus on clustering activity in time characteristic for mass movements, we calculate the detection density over a 5 min sliding window (noise classification is set to 0, and mass movement to 1).

3. To give more weight to the strength of the signal, we multiply the detection density by the root mean square (RMS) of station SPZ03. The RMS is one of the 69 features and is therefore given more weight manually since previous studies showed that the maximum seismic amplitude scales with landslide and rockfall volumes [18, 19]. We use station SPZ03 since the detection results for this station are the most stable.

We now investigate the initial results of mass movement activity at Spitze Stei before two debris flows events that occurred on May 19 ("debris flows 1") and June 27, 2022 ("debris flows 2").
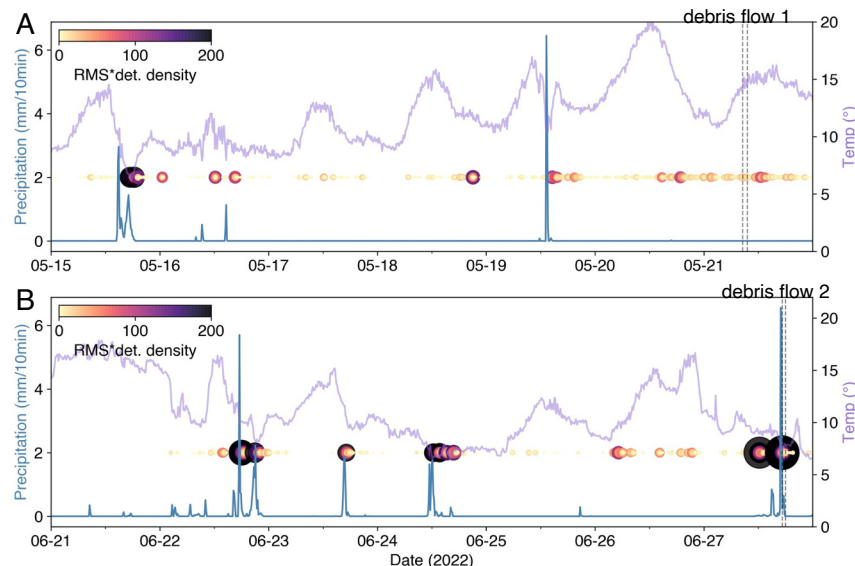
Fig. 3. One-week time series before the debris flows events of the detection density multiplied with the RMS (circles), the precipitation in 10 minutes (blue), and the temperature (purple). Both metrological measurements were made locally at Spitze Stei. Detection density multiplied with the RMS is plotted as a scatter plot. Each circle's color and size correspond to the RMS values multiplied by the detection density. The occurrence of debris flows is represented in black dashed vertical bars

4 Results

Figure 3 shows the initial results of mass movement detection at Spitze Stei through seismic data and machine learning compared with temperature and precipitation measurements. We show results for 6 days preceding the debris flow events that occurred on May 21 (~08:35 UTC, duration ~1 h) and June 27 (~17:18, duration ~40 in), 2022. The start time and duration of

the debris flows were estimated based on camera and discharge data. The first debris flow occurred on a sunny day, was most probably triggered by meltwater from snow deposits, and had a high solid volume fraction. The second debris flow was triggered by rather heavy rainfall of 14 mm h^{-1}.

The metric that we use, RMS multiplied by the detection density, combines the information on the intensity of activity (the more detections in the 5 min time window, the higher the detection density) and the volume of mass movement events. Our results show high mass movement activity on times of high rainfall on 15, 17, and 19 May; and June 22, 23, 24, and 27 June. However, events occurring outside of rainy periods were also detected, for example, on May 16 at 00:33 UTC and May 18 at 21:02 UTC. These two events were confirmed independently with the camera data and can be described as a debris-snow avalanche and debris fall originating from the top of Spitze Stei. The results also show preceding mass movement activity before the debris flow events. Mass movement activity before debris flow 1 is extended, lasting for several hours from May 20, 15:00 UTC, with RMS*det. density values between 50-100. The mass movement activity before debris flow 2 lasts for 15 minutes, between 12:05 and 12:20 UTC on June 27 and with RMS*det. density values between 260-750.

5 Discussion and conclusions

Previous studies showed a direct link between the volume of material accumulated at the base of Spitze Stei and the volume of subsequent debris flows [10]. Only the mass movements at Spitze Stei that reach the slope's terminus supply the material causing debris flows. On the other hand, rock falls, and landslides in the upper part of Spitze Stei do not directly contribute to debris flows. Our method only detects mass movements in time without focusing on their spatial origin or trajectory. In the following steps, the proposed method could be combined with seismic location methods [20] to differentiate between the rockfalls and landslides depositing their material at the slope or below it.

The initial results prove that machine learning combined with seismic approaches can constrain the periods of mass movement activity at Spitze Stei. These mass movements act as primary sediment sources conditioning debris flows activity. Our results show that the mass movement activity at the Spitze Stei rockslide can initiate hours before a subsequent debris flow event. This information might be crucial in mitigating debris flow hazards and extending warning time, especially for debris flows triggered by factors other than precipitation.

References

1. F. Walter, F. Amann, F., A. Kos, R. Kenner, M. Phillips, A. de Preux, M. Huss, C. Tognacca, J.Clinton, T. Diehl, Y. Bonanomi, Geomorphology, **351**, 106933 (2020)

2. DH. Shugar, M. Jacquemart, D. Shean, et al., Science, **373**, 300-306 (2021)

3. W. Tinner, P. Kaltenrieder, M. Soom, P. Zwahlen, M. Schmidhalter, A. Boschetti, C. Schlüchter, EclogaeGeol Helv, **98**, 83–95 (2005)

4. C. Kienholz, R. Riner, K. Graf, D. Tobler, N. Hählen, J. Häberle, FAN-AGENDA, **1**, 54–63 (2021)

5. Geotest, *Kandersteg, "Spitze Stei" Gefahrenmanagement. Bericht Nr. 1418139.2*, Zollikofen (2019)

6. R. Caduff, T. Strozzi, N. Hählen, and J. Häberle, *Accelerating Landslide Hazard at Kandersteg, Swiss Alps; Combining 28 Years of Satellite InSAR and Single Campaign Terrestrial Radar Data*, in Understanding and Reducing Landslide Disaster Risk, edited by V. Vilímek, F. Wang, A. Strom, K. Sassa, P. T. Bobrowsky, and K. Takara, ICL Contribution to Landslide Disaster Risk Reduction, Springer International Publishing, 267–73 (2021)

7. Geotest, *Kandersteg, "Spitze Stei", Sicherheitskonzept Gemeinde, Bericht Nr. 1418139.6*, Zollikofen (2021)

8. R. Kenner, V. Gischig, Z. Gojcic, et al., Landslides, **19**, 1357–1377 (2022)

9. Geotest, *Kandersteg, "Spitze Stei" Gefahrenmanagement. Bericht Nr. 14181391.25*, Zollikofen (2021)

10. Geotest, *Einwohnergemeinde Kandersteg Kandersteg, Oeschibach Dispositionsmodell Murgang Ereignis- und Dispositionsanalyse 2021. Bericht Nr. 14181391.27*, Zollikofen (2022)

11. M. Stoffel and C. Huggel, Progr Phys Geogr, **36**, 421–39 (2012)

12. A. Curtis, P. Gerstoft, H. Sato, R. Snieder, and K. Wapenaar, The Leading Edge, **25**, 1082–1092 (2006)

13. G. Belli, F. Walter, B. McArdell, D. Gheri, D., and E. Marchetti, JGR: Earth Surface, **127**, e2021JF006576 (2022)

14. F. Provost, C. Hibert, and J.-P. Malet, GRL, **44**, 113–120 (2017)

15. M. Wenner, C. Hibert, A. van Herwijnen, L. Meier, and F. Walter, NHESS, **21**, 339–361 (2021)

16. M. Chmiel, F. Walter, M. Wenner, Z. Zhang, B. McArdell, & C. Hibert, GRL, e2020GL090874 (2021)

17. L. Husmann, *Automation of Mass Movement Detection in Seismic Data (Spitze Stei, Switzerland)*, Master Thesis, D-ERDW, ETH Zurich (2023)

18. C. Hibert, A. Mangeney, G. Grandjean, N. M. Shapiro, J. Geophys. Res., **116**, F04032 (2011)

19. M. Farin, A. Mangeney, J. de Rosny, J., R. Toussaint, R., and P.-T. Trinh, JGR: Earth Surface, **124**, 2987-3021 (2019)

20. Chmiel, M., P. Roux, T. Bardainne, Geophysics, **84**, KS211-KS223 (2019)